

RESEARCH PAPER



MiR-597-5p inhibits carcinogenesis and macrophage recruitment in colitis-related colorectal cancer via reducing the expression of CXCL5

Shuo Li^a, Miao Yu^b, Xiuying Wang^c, and Bingyuan Fei^b

^aDepartment of Hepatobiliary and Pancreatic Surgery, China-Japan Union Hospital of Jilin University, Changchun, China; ^bDepartment of Gastrointestinal Colorectal Surgery, China-Japan Union Hospital of Jilin University, Changchun, China; ^cMedical Department, China-Japan Union Hospital of Jilin University, Changchun, China

ABSTRACT

Despite being the subject of multiple cancer studies, nothing is known about miR-597-5p's role in colitis-associated colorectal cancer (CAC). We intend to explore how miR-597-5p influences the growth and development of CAC. In order to construct a CAC model, mice were stimulated with azoxymethane (AOM)/dextran sulfate sodium (DSS). The in situ hybridization (ISH) and quantitative real-time polymerase chain reaction (qRT-PCR) was used for the detection of miR-597-5p expression. The protein expression of CXCL5 was determined by western blotting, immunohistochemistry and enzyme-linked immuno sorbent assay (ELISA). The histologic colitis score and hematoxylin and eosin (HE) staining were used to evaluate degree of damage to colonic tissues. The proportion of macrophages detected in colon tumors was also measured using flow cytometry. The transwell test was employed to assess macrophage migration. It was found that the miR-597-5p and its target CXCL5 had a negative correlation. MiR-597-5p expression was decreased, while CXCL5 expression was raised in CAC tissues. In AOM/DSS-induced mice, miR-597-5p deficiency in intestinal epithelial cells resulted in decreasing colon length as well as increasing tumor numbers and histologic colitis score, which was reversed by CXCL5 inhibition. MiR-597-5p deficiency facilitated macrophage recruitment in AOM/DSS-induced mice and promoted macrophage migration in vitro, which were reversed by CXCL5 inhibition. Deficiency of miR-597-5p aggravated macrophage recruitment and tumorigenesis in a mouse CAC model, suggesting that miR-597-5p agonists may have an anti-inflammatory therapeutic effect in inflammatory bowel diseases and reduce the risk of developing CAC.

ARTICLE HISTORY

Received 18 July 2023
Revised 11 September 2023
Accepted 13 September 2023

KEYWORDS



Colorectal cancer (CRC);
CXCL5; microRNA-597-5p;
Colitis-associated colorectal
cancer (CAC)


Introduction

Colorectal cancer (CRC) refers to a common malignancy of digestive system, and its incidence ranks third among all cancers.¹ There are several distinct carcinogenic routes that can lead to CRC development, including the well-known adenoma-carcinoma sequential pathway (ACSP), the systemic inflammatory pathway (SIP), and the serrated pathway (SP).² Colitis-associated colorectal cancer (CAC) results from unchecked mutated cells growth, which is aided by the SIP.³ CAC accounts for about 5% of CRC cases, which is one of the typical examples of cancers that are closely related to chronic inflammation.^{4,5} Inflammatory diseases of the intestine, Crohn disease (CD) or ulcerative colitis (UC), increases the chances of developing CAC.⁶ Chemotherapy and targeted treatment have helped increase the likelihood of surviving five years for CAC patients, but the outlook is still grim.⁷⁻⁹ Specifically, numerous studies have shown that macrophages hasten the development of immunosuppressive tumor microenvironment (TME),^{10,11} which in turn promotes tumor growth and progression.¹² Thence, targeting macrophages including inhibition of macrophage recruitment and survival may be an efficient strategy for CAC treatment.

MicroRNAs, also known as miRNAs, are non-protein-coding transcripts that consists of 19–24 nucleotides, which inhibit the translation of target messenger RNAs (mRNAs) to control post-transcriptional modulation of gene expression.¹³ MiRNAs have been the subject of much exploration as potential causes of inflammatory and malignant disorders.¹⁴ Multiple miRNAs have been linked to controlling CAC development, for example miR-214, miR-146a and miR-21.¹⁵⁻¹⁷ MiR-597-5p in particular has been associated with regulation of CRC. For instance, miR-597-5p up-regulation suppresses the growth and infiltration of CRC cells.¹⁸ Inhibition of miR-597-5p facilitates CRC cell growth, progression through the cell cycle and development of colonies.¹⁹ However, miR-597-5p's effects on macrophage recruitment and carcinogenesis in CAC are rarely investigated.

C-X-C motif ligand 5 (CXCL5) is a critical chemokine in inflammatory TME.²⁰ It belongs to the CXC family, which functions as the ligand for CXCR2 to affect tumor growth and metastasis.^{21,22} Substantial evidence indicates a possible function for CXCL5 in CRC. For instance, CXCL5 is proved to facilitate migration and invasion of tumor cells in CRC.^{23,24} CXCL5 is demonstrated to induce tumor angiogenesis through

CONTACT Bingyuan Fei  feibingyuan@jlu.edu.cn  Department of Gastrointestinal Colorectal Surgery, China-Japan Union Hospital of Jilin University, No.126 Xiantai Street, Changchun 130033, China

 Supplemental data for this article can be accessed online at <https://doi.org/10.1080/15384047.2023.2274122>

© 2023 The Author(s). Published with license by Taylor & Francis Group, LLC.

This is an Open Access article distributed under the terms of the Creative Commons Attribution-NonCommercial License (<http://creativecommons.org/licenses/by-nc/4.0/>), which permits unrestricted non-commercial use, distribution, and reproduction in any medium, provided the original work is properly cited. The terms on which this article has been published allow the posting of the Accepted Manuscript in a repository by the author(s) or with their consent.

enhancing the expression of FOXD1 in CRC.²⁵ However, it is unknown exactly how miR-597-5p controls CXCL5 in CAC.

This study aimed at investigating the influence of miR-597-5p on CAC growth and macrophage recruitment, and the pathway through which miR-597-5p exerts its regulatory effects on CAC was investigated.

Results

The target of miR-597-5p is CXCL5

To identify potential targets for miR-597-5p, we queried the Targetscan database. As can be shown in Figure 1a, the 3' untranslated region of CXCL5 contained miR-597-5p recognition sequences, suggesting that miR-597-5p showed potential to target CXCL5. Then overexpression or inhibition of miR-597-5p in Caco2 cells was conducted. As expected, miR-597-5p showed high expression upon introducing the miR-597-5p mimic by transfection, and showed low expression upon transfection of miR-597-5p inhibitor ($P < .01$, Figure 1b, c). We next focused on their regulatory relation. Following up-regulation of miR-597-5p expression in Caco2 cells, a substantial decrease in CXCL5 mRNA and protein levels was observed ($P < .01$, Figure 1d-g), but it was significantly increased when miR-597-5p expression was suppressed.

A reduction in miR-597-5p expression and an elevation in CXCL5 expression were observed in CAC tissues

For analyzing miR-597-5p expression, colonic tissues were collected from azoxymethane (AOM)/dextran sulfate sodium (DSS)-induced mice at the end of the 0th, 2th, 6th, 10th and 18th weeks after AOM/DSS treatment. According to data from in situ hybridization (ISH) assay (Figure 2a) and qRT-PCR (Figure 2b, $P < .01$), it was observed that miR-597-5p expression level was decreased in mouse colonic tissues collected at the termination of weeks 2, 6, 10 and 18 after AOM/DSS treatment compared to mouse colonic tissues collected at the end of the 0th week following AOM/DSS treatment. Moreover, protein expression of CXCL5 was detected in AOM/DSS-induced colonic tissues. Data from IHC staining (Figure 2c) and western blot (Figure 2d, $P < .05$) consistently demonstrated that CXCL5 expression was boosted in mouse colonic tissues collected at completion of the 2th, 6th, 10th and 18th weeks compared to mouse colonic specimen collected at the end of the 0th week after AOM/DSS administration.

We also collected colonic mucous samples from non-IBD /CRC patients (controls) and neoplastic mucous samples from patients with UC, CD and CRC to assess miR-597-5p and CXCL5 expression. We used ISH and qRT-PCR ($P < .01$) to

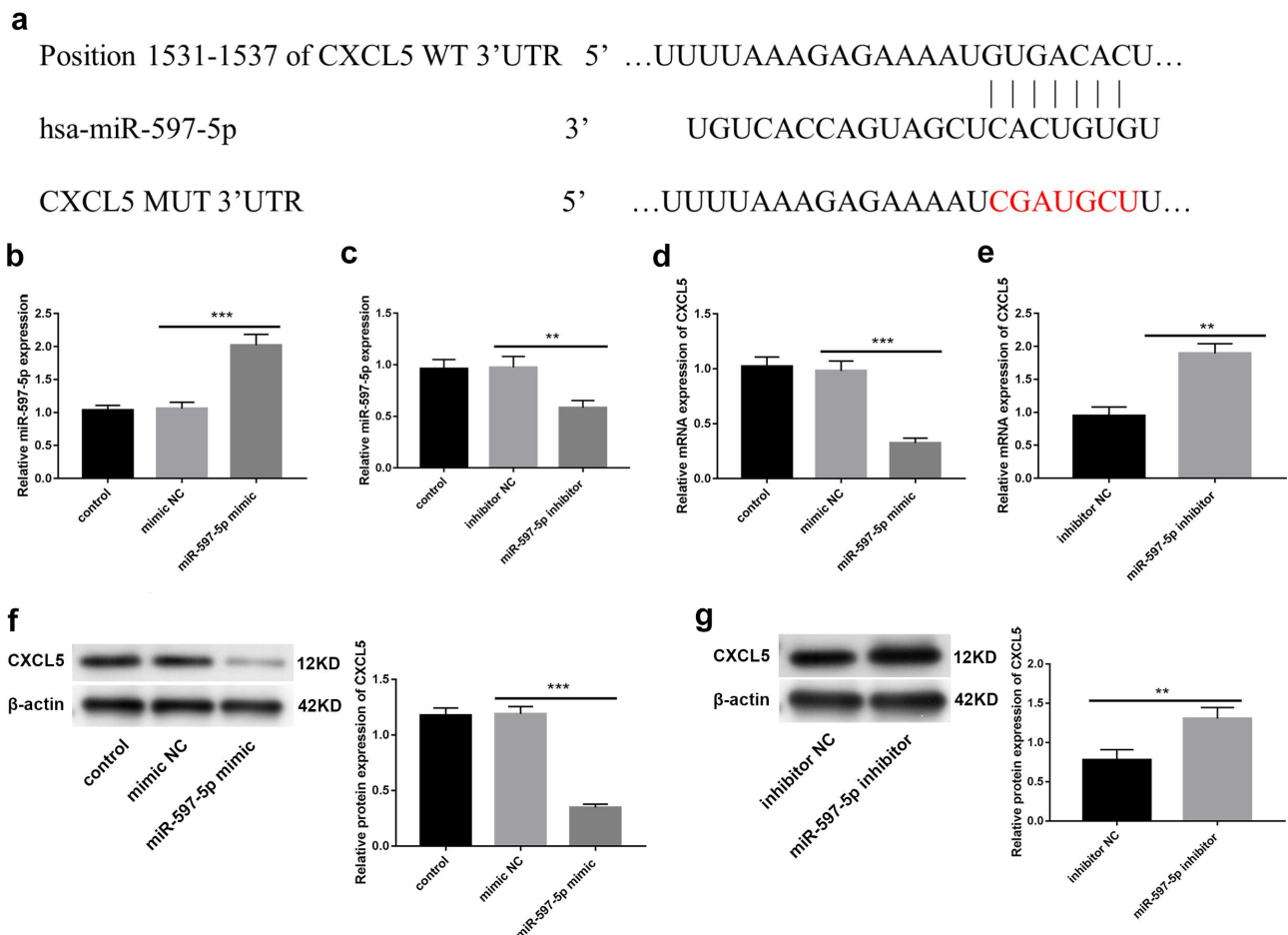


Figure 1. The miR-597-5p exerts direct regulation on CXCL5 by targeting its mRNA. (a) predictive analysis using Targetscan database revealed the putative targets of miR-597-5p. (b-c) after transfecting miR-597-5p mimic/inhibitor, miR-597-5p levels in Caco2 cells were quantified by performing qRT-PCR analysis. (d-e) relative mRNA expression of CXCL5 in Caco2 cells was assessed through qRT-PCR analysis. (f-g) relative expression of protein of CXCL5 in Caco2 cells was quantified by western blot. ** $P < .01$, *** $P < .001$. Samples were assessed in triplicate.

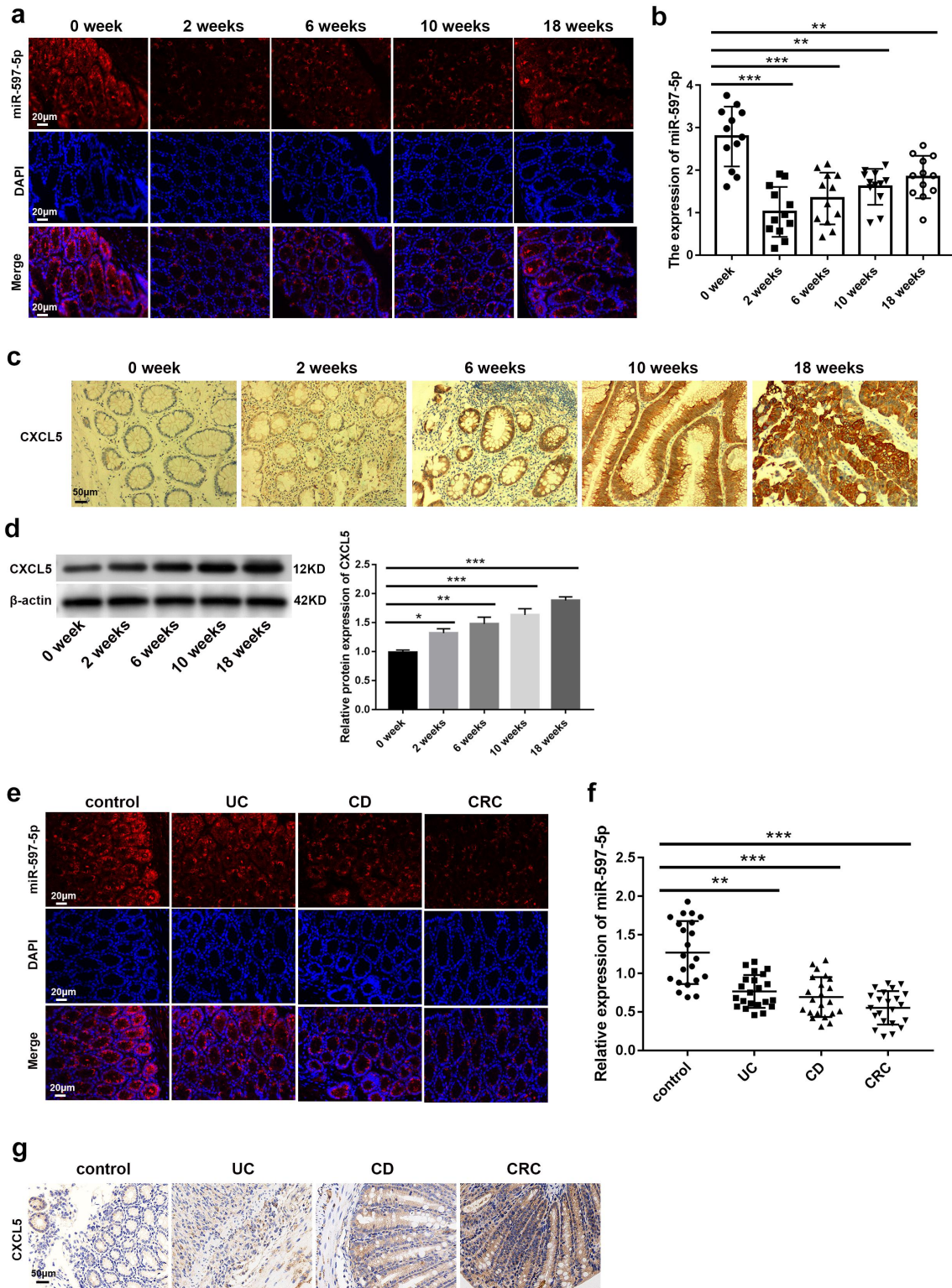


Figure 2. MiR-597-5p expression was decreased and CXCL5 expression was increased in CAC tissue-specimen. (a) MiR-597-5p expression in colonic samples of AOM/DSS-induced mice was determined using in situ hybridization (ISH). $N = 6$. (b) quantification of miR-597-5p expression in colonic tissues of mice following AOM/DSS treatment was done via qRT-PCR. $N = 12$. (c) the protein expression of CXCL5 in colonic tissues of AOM/DSS-induced mice was detected by immunohistochemical (IHC) staining. $N = 6$. (d) the protein level of CXCL5 in colonic specimen of AOM/DSS-treated mice was detected by western blot. $N = 6$. (e) MiR-597-5p in colon mucosa of patients with non-IBD/CRC and tumor mucosa of UC, CD and CRC patients was detected by ISH. $N = 6$. (f) MiR-597-5p expression in colon-mucosa of patients without inflammatory bowel disease/non-colon cancer (non-IBD/CRC) (control) as well as tumor mucosa of ulcerative colitis (UC), Crohn's disease (CD) and CRC patients was detected via qRT-PCR. $N = 22$. (g) the CXCL5 protein expression in colon specimen of patients without IBD/CRC as well as tumor mucosa of UC, CD and CRC patients was detected by IHC staining. $N = 5$. * $P < .05$, ** $P < .01$, *** $P < .001$.

demonstrate that miR-597-5p expression was evidently less in UC, CD, and CRC samples as opposed to controls (Figures 2e, f). Compared to control samples, UC, CD, and CRC patient specimens exhibited increasing protein expression of CXCL5 (Figure 2g).

The deletion of miR-597-5p in IECs accelerates early tumor development and promotes CXCL5 expression in mice treated with AOM/DSS

To understand the impact of miR-597-5p on CAC initiation and progression, histological changes of miR-597-5p^{IEC/-} mice were monitored following the completion of the 0, 2th, 6th, 10th, and 18th weeks since the initiation of AOM/DSS treatment. The repetitive cycles of epithelial injury and subsequent healing elicited by DSS exposure led to the hypertrophy of the smooth muscle layer within the mucosa and deposition of extracellular matrix (ECM), which played a role in the observed shortening of the affected area.²⁶ We observed that miR-597-5p^{IEC/-} led to reduction of mouse colon length at the end of the 2th week after AOM/DSS induction as shown in Figure 3a ($P < .01$). Meantime, the increased number of macroscopically visible tumors was observed in colonic specimens of miR-597-5p^{IEC/-} mice at the end of the 18th week after AOM/DSS induction ($P < .01$, Figure 3b–c). The mean scores for histological colitis in miR-597-5p^{IEC/-} mice exhibited an increase in comparison to wild-type mice ($P < .01$, Figure 3d). As displayed in Figure 3e, miR-597-5p^{IEC/-} mice exhibited severe damage of epithelial barrier at the completion of the second week after induction with AOM/DSS, and many inflammatory cells infiltrated colonic mucosa and submucosa. Upon reaching the 6th week following AOM/DSS treatment, miR-597-5p^{IEC/-} mice showed inflammatory hyperplasia and dysplasia crypt in colonic tissues. After the completion of 10 weeks of AOM/DSS induction, persistent recurrent inflammation with alternating periods of exacerbation and remission expedited the progression of aberrant crypt foci and dysplasia. At the conclusion of 18th week of AOM/DSS induction, advanced-stage intra-epithelial neoplasia and carcinoma polyp were observed in miR-597-5p^{IEC/-} mice. In a word, miR-597-5p^{IEC/-} resulted in severer colonic inflammation of AOM/DSS-induced mice, promoting CAC development.

Furthermore, we discovered that protein expression of CXCL5 was raised in response to miR-597-5p deletion in AOM/DSS-induced mice according to data from IHC staining (Figure 3f) and ELISA ($P < .01$, Figure 3g).

The CXCL5/CXCR2 inhibitor (SB225002) decreases mucosal impairment and prolongs the initiation of dysplasia in miR-597-5p-deficient mice

Next, SB225002 (anti-CXCL5) was injected into AOM/DSS-induced miR-597-5p^{IEC/-} mice to investigate the influence of CXCL5 on the initial phases of CAC development. It was revealed that the colon length was increased by injection of anti-CXCL5 in Figure 4a ($P < .05$) and the tumor number was reduced by injection of anti-CXCL5 in AOM/DSS-induced miR-597-5p^{IEC/-} mice ($P < .001$, Figure 4b). Besides, the average colitis scores based on histopathological evaluation of

AOM/DSS-induced miR-597-5p^{IEC/-} mice were decreased by injection of anti-CXCL5 ($P < .05$, Figure 4c). Also, histological analysis indicated that anti-CXCL5 mitigated inflammation-induced damage and early progression of neoplasia and dysplasia in colonic specimen of AOM/DSS-induced miR-597-5p^{IEC/-} mice (Figure 4d).

MiR-597-5p inhibition facilitates macrophage recruitment and chemotaxis through up-regulating CXCL5

Finally, the influences of miR-597-5p or CXCL5 on macrophage recruitment and chemotaxis were explored. It was demonstrated that the level of CD68 positive phagocytic cells in lamina propria of mice subjected to AOM/DSS treatment were increased after miR-597-5p deficiency, but the promoting impact of miR-597-5p deficiency on CD68+ macrophages was counteracted by anti-CXCL5 (Figure 5a). Besides, the proportion of macrophages in either lamina propria or peritoneal lavage of miR-597-5p^{IEC/-} mice was increased relative to that of wild-type mice, but was reduced by anti-CXCL5 in AOM/DSS-induced miR-597-5p^{IEC/-} mice especially at the conclusion of week-18 after AOM/DSS induction ($P < .05$, Figure 5b,c).

Caco2 cells overexpressing miR-597-5p or inhibiting miR-597-5p were co-cultured with macrophages (THP-1 cells) to explore the impact of miR-597-5p and CXCL5 on monocyte chemotaxis. When co-cultured with miR-597-5p-overexpressed Caco2 cells, the number of migrated macrophages was distinctly reduced while evidently boosted after addition of exogenous rCXCL5 ($P < .01$, Figure 5d). When co-cultured with miR-597-5p-inhibited Caco2 cells, the population of migrated macrophages was substantially boosted while markedly reduced after addition of anti-CXCL5 ($P < .05$, Figure 5d).

Discussion

As a malignant colonic tumor with high mortality rate, increasing people are committed to investigating potential pathogenesis mechanisms of CAC for developing new therapeutic agents.^{27–29} And the CAC mouse model created by AOM/DSS has been used in a wide variety of research projects.^{30,31} In the present study, it was discovered that the miR-597-5p displayed lower expression in mouse colonic tissues collected at the completion of week 2, 6, 10 and 18 of AOM/DSS treatment than mouse colonic tissues collected at the end of the 0th week after AOM/DSS administration. Meantime, we also observed lower miR-597-5p expression in carcinoma mucosa from UC patients, CD patients and CRC patients than that in colonic mucosa samples from non-IBD/CRC patients. The miR-597-5p expression trend in our results was in line with prior work, which reported that miR-597-5p expression was distinctly decreased in CRC cells.^{18,19} These results provided more evidence that miR-597-5p may contribute to CAC's etiology.

Previous studies have linked IECs to the development of CAC.^{32,33} It has also been shown that miR-597-5p has a major impact on CRC. For instance, epithelial-mesenchymal transformation (EMT) and invasion of CRC cells are repressed by

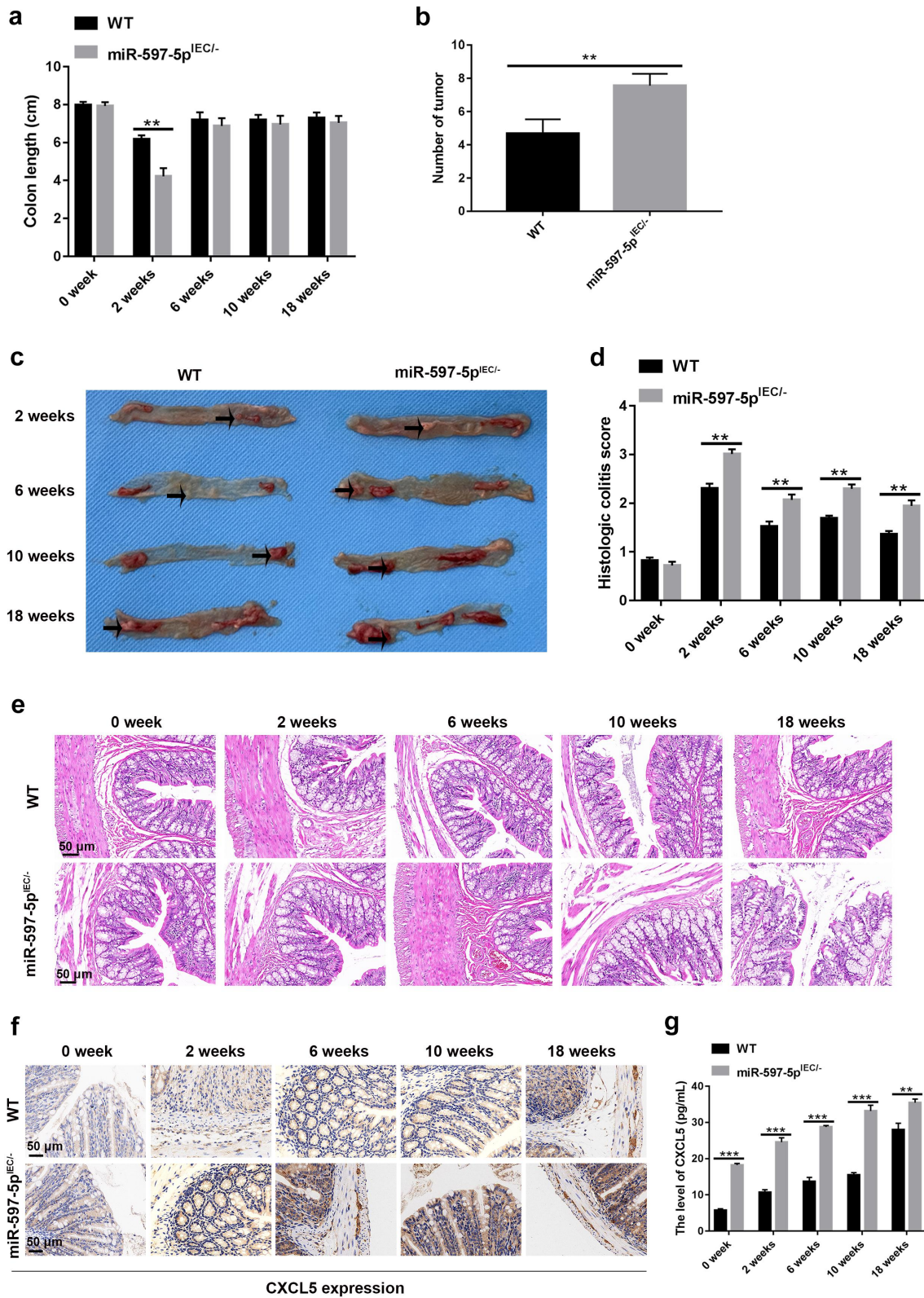


Figure 3. The miR-597-5p-deletion in intestinal epithelial cells (IECs) accelerates CAC early development and promotes CXCL5 expression in AOM/DSS-treated mice. (a) the colon length of mice was gauged. *N* = 3. (b) the number of tumors was calculated at the completion of 18th week of AOM/DSS introduction. *N* = 6 (c) gross colon morphology conclusion of the 2th, 6th, 10th and 18th weeks following AOM/DSS treatment. *N* = 3. (d-e) histological colitis scores of mice and representative images of histological sections in each group. *N* = 3. (f) Immunohistochemical (IHC) staining was employed for the detection of protein expression of CXCL5 in colonic tissues of AOM/DSS-induced mice. *N* = 6. (g) ELISA was used to detect the presence of CXCL5 protein in the supernatant of mouse colonic specimen. *N* = 3. ***P* < .01, ****P* < .001.

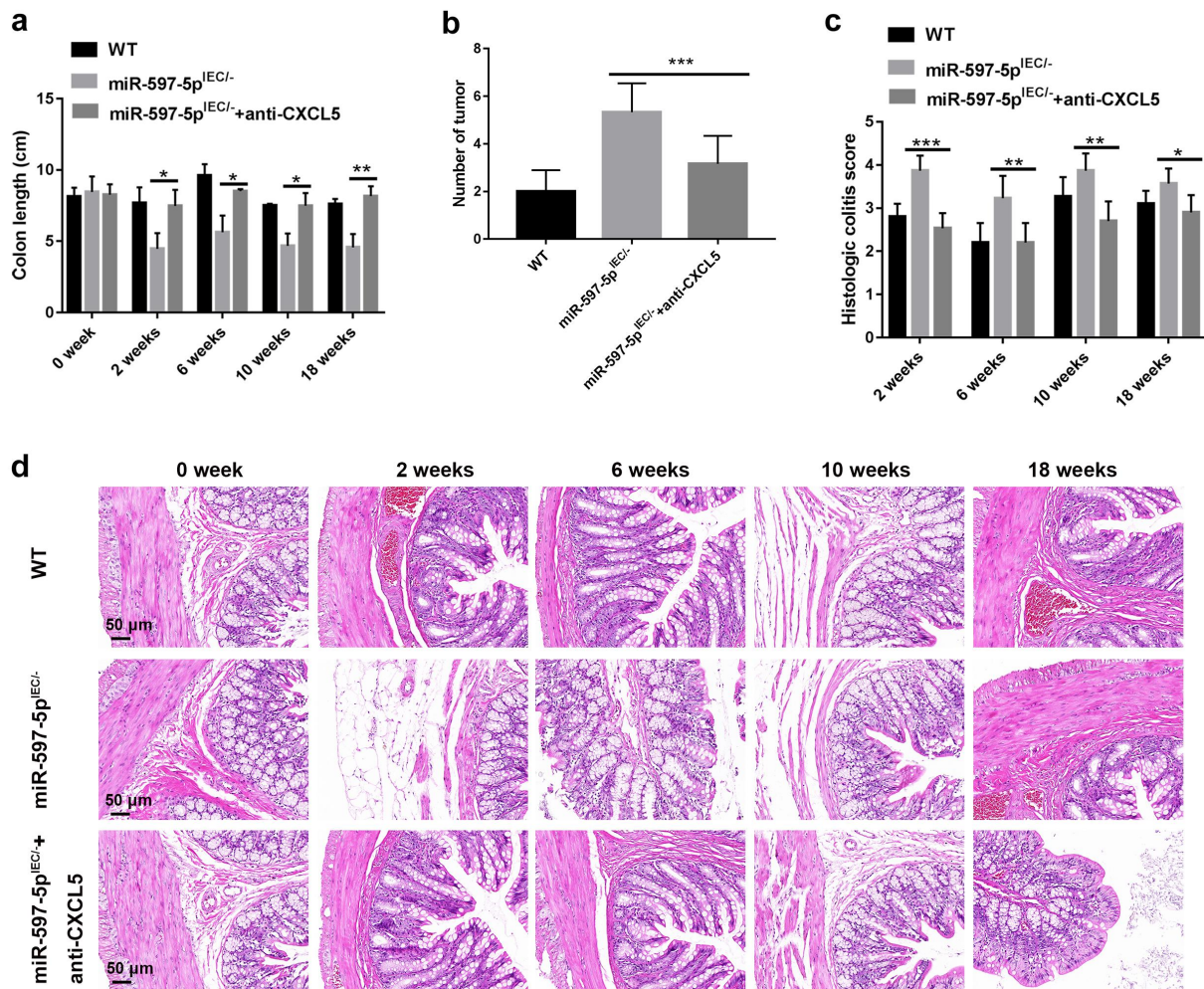


Figure 4. CXCL5 antibody attenuates mucosal injury and slows down the development of neoplasia in AOM/DSS-treated miR-597-5p^{IEC/-} mice. (a) the colon length of mice was gauged. $N=3$. (b) the number of tumors was calculated after 18 weeks of AOM/DSS exposure. $N=6$. (c-d) histological colitis scores of mice and representative images of histological sections in each group. $N=3$. * $P < .05$, ** $P < .01$, *** $P < .001$.

overexpression of miR-597-5p.¹⁸ MiR-597-5p suppression facilitates colony formation, cellular growth and cell cycle regulation of CRC cells.¹⁹ For this reason, we engineered an AOM/DSS-induced miR-597-5p^{IEC/-} mice model to probe miR-597-5p's role in CAC. Similar to previous studies showing that miR-597-5p has an anti-tumor effect in CRC, we discovered that miR-597-5p ablation in IECs worsened colon inflammatory conditions, mucosal damage and regression in AOM/DSS-induced mice, aggravating development of CAC. Given the importance of macrophages in CRC microenvironment,³⁴⁻³⁶ we investigated miR-597-5p's role in this process. It turned out that miR-597-5p deficiency in IECs promoted the recruitment of macrophages in AOM/DSS-induced mice, and miR-597-5p suppression facilitated migration of macrophages in co-cultured system of macrophages and Caco2 cells. Considering all above findings, we inferred that miR-597-5p exerted a protective influence in IECs during CAC development, and miR-597-5p agonist may be a potential application in CAC alleviation.

There is evidence that miRNAs exert their functions via binding to target genes.^{37,38} Here, we discovered that miR-597-5p selectively targeted and regulated CXCL5 gene expression. Abundant researches have suggested that CXCL5 is highly expressed in the inflammatory colon and CRC.^{24,25,39}

Consistently, we observed up-regulation in CXCL5 expression in colonic specimens of AOM/DSS-induced CAC mice as well as UC, CD and CRC patients. At the same time, we discovered that miR-597-5p negatively regulated CXCL5 expression in Caco2 cells. When CXCL5 inhibitor was added, miR-597-5p deletion-induced mucosal damage and dysplasia was alleviated. Meanwhile, the promoting effects of miR-597-5p down-regulation on recruitment and migration of macrophages were reversed by CXCL5 inhibitor. Combining these findings, we deduced that miR-597-5p impaired early development of CAC and macrophage recruitment through reducing CXCL5 expression in AOM/DSS-induced mice. However, a limitation of this study is the difference in sample size and relatively small sample size. In future investigation, we will use more samples to perform experiments.

In summary, miR-597-5p was lowly expressed in colonic tissues of AOM/DSS-induced mice as well as carcinoma mucosa samples from UC patients, CD patients and CRC patients. MiR-597-5p deficiency facilitated progression of colitis and CAC in AOM/DSS-induced mice, and contributed to recruitment and chemotaxis of macrophages. Mechanistically, miR-597-5p repressed early development of CAC, which may be associated with CXCL5.

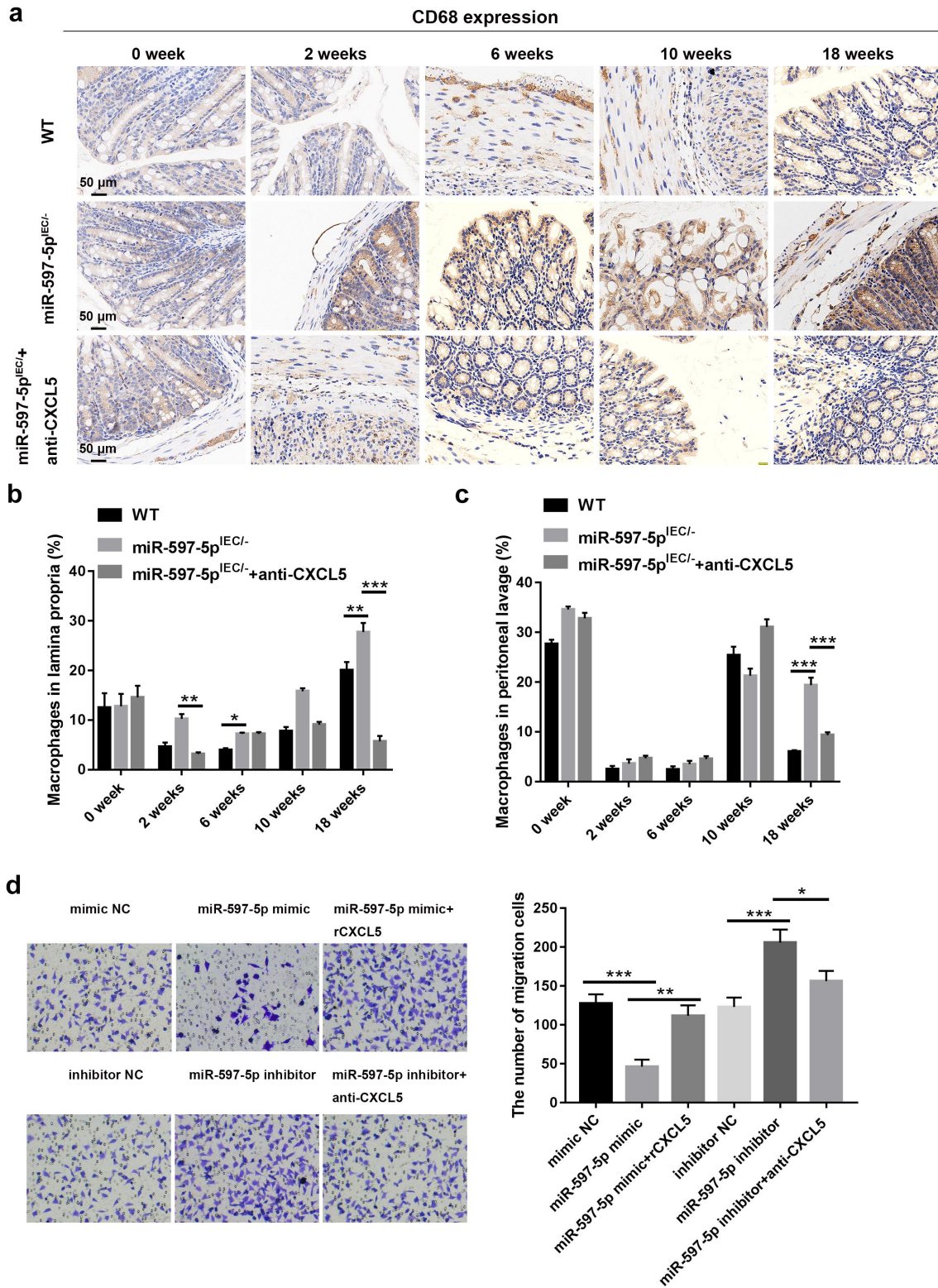


Figure 5. MiR-597-5p down-regulation facilitates macrophage recruitment and migration through up-regulating CXCL5. (a) visual representations of IHC staining for CD68 in colonic specimen of mice subjected to AOM/DSS treatment. $N = 3$. (b-c) quantification of colonic macrophages in the lamina-propria/peritoneal lavage samples derived from mice at specific time points (0th, 2th, 6th, 10th, and 18th weeks) post AOM/DSS treatment using flow cytometry analysis. Two-parameter histograms of F4/80+CD11b+ were recognized as macrophages and quantified. $N = 3$. (d) migration potential of macrophages was determined using the transwell migration assay. Samples were examined in triplicate. * $P < .05$, ** $P < .01$, *** $P < .001$.

Material and methods

Cell culture

The Cell Repository of the Chinese Academy in Shanghai, China facilitated the provision of a human CRC cell line (Caco2) and a human monocytic cell line (THP-1). THP-1 cells grew in RPMI 1640 (HyClone Christchurch, MA, USA) mixed with 10% fetal bovine serum (FBS) derived from neonatal calves, streptomycin solution at a concentration of 100 mg/mL and penicillin solution at a concentration of 100 U/mL, while Caco-2 cells grew in DMEM (HyClone Marlborough). All cells were maintained at 37°C, 5% CO₂ and 95% humidity. To promote differentiation into M0 macrophages, THP-1 cells were subjected to treatment with 150 nanomolar (nM) concentration of phorbol 12-myristate 13-acetate, abbreviated as PMA (Sigma Aldrich, St. Louis, MO, USA) for 48 h.

Cell transfection

The miR-597-5p mimic and inhibitor along with mimic negative control (NC) and inhibitor NC were procured from RiboBio (Guangzhou China). Caco2 samples were seeded at a rate of 3×10^5 cells/well in six-well plates. Transfection of the cells was performed when they reached 70% confluence, utilizing synthetic mimic of miR-597-5p (50 nM), mimic NC (50 nM), miR-597-5p inhibitor (100 nM), or inhibitor NC (100 nM) in conjunction with Lipofectamine 3000 (Invitrogen, Carlsbad, California, USA). Following transfection of 48 h, cells were collected for analysis.

The term “quantitative real-time polymerase chain reaction” is denoted by the acronym “qRT-PCR”

RNA was extracted utilizing TRIzol reagent (Invitrogen), followed by quantification using UV spectrophotometry. The extracted RNA reverse transcribed into cDNA with the use of a First-Stand cDNA Creation SuperMix kit (TransGen, Beijing, China). After that, PCR amplification was conducted following the protocols provided a SYBR Premix Ex Taq kit (Takara, Dalian, China). The reaction was carried out under these conditions: an initial denaturation step at 94°C for 5 min, subsequently, a total of 30 amplification cycles were performed, consisting of denaturation at 94°C for 30 seconds, annealing at 55°C for 25 s, and extension for 72°C for 60 s. Primer sequences from the Sangon (Shanghai, China) were included in Table 1. Relative expression of miR-597-5p and CXCL5 mRNA were determined using the $2^{-\Delta\Delta Ct}$ method, standardized by U6 or GAPDH.

Western blotting

For protein extraction, Caco2 cells and tissue samples were treated with “RIPA lysis buffer (Beyotime, Shanghai, China)”, and protein quantity was assessed utilizing a Pierce BCA Protein-Assay-kit (PAT) sourced from Thermo Fisher Scientific (Waltham, MA, USA). Subsequently, 50 µg proteins were exposed to 10% sodium dodecyl sulfate-polyacrylamide gel electrophoresis, and then moved to polyvinylidene fluoride filters (Millipore, Temecula, USA). Prior to blocking with 5% skimmed milk, overnight incubation of the membranes at 4°C was conducted with primary antibodies directed against CXCL5 and β-actin (diluted to 1:1000; ab305100 & ab213262; Abcam, Cambridge, USA). Next, the diluted anti-rabbit secondary antibody diluted at 1:2000 (ab6721, Abcam) was appended to incubate for 1 h. Finally, we used Image J to quantify proteins after examining protein blots with a Bioimaging workstation (BioRad, Berkeley, California, USA).

Establishment of a CAC mouse model

From the Scientific Animal Centre at Guangzhou’s Southern Medical University, we purchased male mice of the C57BL/6 strain, aged 8–10 weeks. The mice were exposed to a controlled environment at $25 \pm 2^\circ\text{C}$ and the light/dark cycle was regulated at 12 h each. The animal care committee at Jilin University (KT20230210) gave their consent to this experiment, and experimental procedures conformed to guidelines for care and use of laboratory animals published by the NIH (revised in 1996).

AOM/DSS was used in accordance with known protocols⁴⁰ to create a CAC mouse model. In brief, mice were administered with AOM (10 mg/kg, Sigma-Aldrich) through intraperitoneal injection. After the initial 7-days AOM administration, mice were given drinking water supplemented with 1.5% DSS (MP Biomedicals, Santa Ana, CA, USA) for another week, and then switched to regular water for a period of two weeks. This cycle was replicated thrice, and from then on, mice were supplied with usual water until the 18th week.⁴¹ For interfering with the CXCL5/CXCR2 axis, were treated with an intraperitoneal injection of a CXCL5/CXCR2 inhibitor (SB225002; MedChemExpress, New Jersey, USA) at a dosage of 2 mg/kg per day. Finally, mice anesthetized with pentobarbital sodium were sacrificed at the end of 0th, 2th, 6th, 10th and 18th weeks. We determined the colon length and the size of the cancer.

Clinical samples

The control samples were collected from colonic mucosa of the non-IBD/CRC patients ($n = 22$), including patients with

Table 1. Primer sequences for qRT-PCR in this study.

Genes		Sequences (5'~3')
miR-597-5p	Forward	5' -ACACTCCAGCTGGGTGTGTCACTCGATGAC-3'
	Reverse	5' -TGGTGTCTGGAGTGC-3'
U6	Forward	5' -CTCGCTTCGGCAGCAC-3'
	Reverse	5' -CTCGCTTCGGCAGCAC-3'
CXCL5	Forward	5' -GCCTCCCTGAACGGGAAG-3'
	Reverse	5' -CAGTTTTCTTGTTCACCGTCCA-3'
GAPDH	Forward	5' -GGACCTGACCTGCCGTCTAG-3'
	Reverse	5' -GTAGCCCAGGATGCCCTTGA-3'

ruptured or obstructed intestinal and volvulus. Carcinoma mucosa samples collected from patients with UC ($n = 22$), CD ($n = 22$) and CRC ($n = 22$) underwent surgical resection. Informed written approval was provided by all participants. Our research was in accordance with the Helsinki Declaration standards and approved by the Health Ethics Committee of China-Japan Union Hospital of Jilin University (2023-KYYS-021).

Mice without intestinal epithelial cells (IECs)-specific miR-597-5p

For generating IECs-specific miR-597-5p-deficient (miR-597-5p^{IEC/-}) mice (Supplemental Figure S1), the recombination systems based on Cre/loxP and Flp/FRT technology (made available by the Shanghai Model Organisms Center, Shanghai, China) were employed for the treatment of C57BL/6 mice. In brief, ES cell-specific gene targeting techniques were utilized to generate miR-597-5p^{flox_{Neo}/+} mice by specifically targeting exon 1 of miR-597-5p. To obtain miR-597-5p^{fl/+} mice, the miR-597-5p^{flox_{Neo}/+} mice were then crossed with Flp transgenic mice (The Jackson Laboratory, Bar Harbour, ME, USA) to delete the Neo cassette. For generating miR-597-5p^{IEC/-} mice, crossbreeding was carried out between miR-597-5p^{fl/+} mice and Villin-Cre transgenic mice (The Jackson Laboratory). The mice were kept in a germ-free environment to ensure sterility.

In situ hybridization (ISH)

ISH was employed to check miR-597-5p expression through digoxigenin (DIG)-labeled miRNA probes. After the tissue was dewaxed and rehydrated, 20 µg/mL proteins K (Servicebio Technology, Wuhan, China) was administered to the slices of colon for 20 min. DIG-labeled miR-597-5p probes were then used for hybridization. After washing with SSC buffers (Servicebio Technology), tissue sections were exposed to inhibitory agent (rabbit serum, Servicebio Technology) during the incubation period. For a duration of 50 min, followed by Cy3-tyramide signal enhancement for 5 min and DAPI staining for 8 min. Anti-fluorescence quenching solutions were used for all tissue sections before they were placed on slides.

Immunohistochemistry (IHC) staining

Tumor tissues immersed in paraffin were sectioned into 4-µm-thick sections, followed by deparaffinization with xylene and subsequent hydration with alcohol. Antigen retrieval was achieved by subjecting the samples to heat treatment in a pre-boiling buffer, followed by block of nonspecific sites with goat serum (Solarbio, Beijing, China). Afterwards, tissue sections were subjected to the primary antibody reaction using anti-CXCL5 (1:500; Cat: DF9919, Affinity, Beijing, China) and anti-CD68 (1:8000; ab213363, Abcam) at 4°C throughout the night. The rabbit-specific antibody (1:500, ab6112, Abcam) was then added to tissue sections and incubated for 30 min, followed by visualization utilizing 3,3'-diaminobenzidine (DAB, Solarbio). We then counterstained with hematoxylin and examined the sections under an Olympus optical microscope (Tokyo, Japan).

Hematoxylin-eosin (H&E) staining

The colon tissues from the mice were incorporated in paraffin, which was fixed in 4% the substance, and dried in a series of ethanol concentrations before cutting them at a thickness of 5 µm. The specimens were then H&E stained after being dewaxed. To capture images of the stained sections, we used a B×50bioluminescent substances microscope (Olympus, Tokyo, Japan).

For evaluating tissue morphological changes, tissue sections were scored according to the following criteria:⁴² inflammatory cell infiltration (graded as 0 = no infiltration, 1 = mild mucosal infiltration, 2 = moderate mucosal and submucosal infiltration and 3 = marked transmural infiltration) was added to the intestinal architecture (0 = no ulceration, 1 = focal erosions, 2 = erosions ± focal ulcerations, 3 = extended ulcerations ± granulation tissue ± pseudopolyps) for a final score with six possible values.”

Enzyme-linked immunosorbent assay (ELISA)

Tissue samples taken from the colon were homogenized in Eppendorf tubes for 1 min. After centrifugation, the supernatant was obtained from the samples for ELISA testing based on instructions of a mouse CXCL5 ELISA kit (YANKANG BIO, Shanghai, China).

Isolation and flow cytometry analysis of colonic lamina propria lymphocytes (LPLs)

The mice intestines were sectioned into 0.5 cm segments, followed by shake with HBSS and 2% FBS. Then intestinal epithelial cells were washed using HBSS for removing epithelial cells. In order to isolate (IELs) of the lamina propria, intestinal specimens were subjected to enzymatic digestion using complete RPMI-1640 medium supplemented with collagenase D (1 mg/mL), Dispase II (40 µL/mL) and DNase I (4 µL/mL) at 37°C. Later on, these samples underwent filtration using a cellular device (BD Biosciences, Franklin Lakes, NJ, USA) until connective tissue was invisible. Subsequently, dissociated cells were rinsed two times with PBS, suspended again in 40% Percoll, layered beneath 80% Percoll and subjected to centrifugation for 20 min. IELs of the lamina propria were obtained from the inter-phase of the Percoll gradient and followed by re-suspension in FACS buffer containing HBSS solution with sodium azide (0.05%) and FBS (3%).

Next, isolated lamina propria IELs of the were subjected to staining with anti-mouse F4/80 antibody conjugated with PE (Cat. no. 565410; BD Biosciences) and CD11b-labeled-FITC (Cat. no. 557396; BD Biosciences) along with their corresponding fluorochrome-conjugated negative control antibodies (Cat no. 553930 and Cat no. 553988; BD Biosciences). Finally, a “BD FACS CANTO II flow cytometer” was employed to analyze cells.

Macrophage-colon cell co-culture system

Caco2 cells (1×10^5 cells per well) transfected with mimics and inhibitors of miR-597-5p along with NC mimic and inhibitor

were seeded into the bottom chamber of the transwell system (8.0 μm pore; Merck Millipore, Burlington, MA, USA) in a 24-well plate. At the same time, THP-1-differentiated phagocytes (2×10^5 cells per well) were added to the upper compartment of transwell system. Following 48 h of co-culture, transwell inserts containing THP-1-differentiated macrophages were introduced into another 24-well plate containing pre-seeded Caco2 cells (1×10^5 cells per well) that had been plated 24 h earlier.

Transwell assay

The chemotactic influence of CXCL5 and miR-597-5p-overexpressed/miR-597-5p-silenced colon cells on phagocytic cells was investigated through a transwell migration assay. In brief, upper chambers of 24-well dishes (Merck Millipore) were seeded with THP-1-differentiated macrophages at a rate of 2×10^5 cells/well in culture medium devoid of FBS. The 600 μL of RPMI 1640 medium containing 15% FBS was introduced into the bottom area together with human recombinant CXCL5 protein (rCXCL5) (PERFEMIKER, Shanghai, China), CXCL5/CXCR2 inhibitor (SB225002; MedChemExpress) or transfected Caco2 cells as chemotactic signals. Following a 24-h incubation period, macrophages adhering to bottom of the chambers were fixed through paraformaldehyde (4%) and stained via crystal violet (0.1%). The migrated macrophages were quantified using an inverted microscope.

Statistical analysis

The mean value along with the standard deviation was reported to represent the experimental data. Data analysis was implemented with the help of GraphPad Prism version 7.0. The tested significance between two groups of data was determined using Student t-test. One-way ANOVA, along with Tukey's test, was employed to compare differences among multiple groups of data. A significance level of $P < .05$ was used to determine statistical significance.

Disclosure statement

No potential conflict of interest was reported by the author(s).

Funding

The author(s) reported there is no funding associated with the work featured in this article.

Notes on contributors

Shuo Li received her PhD degree in surgery from Jilin University in 2015. Now, she is a doctor in China-Japan Union Hospital of Jilin University. Her research focuses on treatment of hepatic diseases.

Dr. Miao Yu is a Gastrointestinal surgeon. She received her PhD from Jilin University in 2020. She specializes in the diagnosis and treatment of common diseases in gastrointestinal surgery.

Xiuying Wang received her BS degree in Clinical Medicine from Norman Bethune Medical University. Now, she is a medical record manager in

China-Japan Union Hospital of Jilin University. Her research focuses on the Medical record management of gastrointestinal related diseases.

Bingyuan Fei received her PhD degree in surgery from Jilin University in 2016. Now, she is a doctor in China-Japan Union Hospital of Jilin University. Her research focuses on treatment of colorectal diseases.

ORCID

Bingyuan Fei  <http://orcid.org/0000-0001-5336-0470>

Authors' contributions

SL and BYF designed the study, MY collected the data, XYW and BYF analyzed the data, SL wrote the manuscript. All authors read and approved the final manuscript.

Data availability statement

The datasets used and analyzed during the current study are available from the corresponding author on reasonable request.

Ethics

Informed written approval was provided by all participants. Our research was in accordance with the Helsinki Declaration standards and approved by the Health Ethics Committee of China-Japan Union Hospital of Jilin University (2023-KYYS-021).

The animal care committee at Jilin University (KT20230210) gave their consent to this experiment, and experimental procedures conformed to guidelines for care and use of laboratory animals published by the NIH (revised in 1996).

References

1. Siegel RL, Miller KD, Fedewa SA, Ahnen DJ, Meester RGS, Barzi A, Jemal A. Colorectal cancer statistics, 2017. *CA Cancer J Clin.* 2017;67(3):177–193. doi:10.3322/caac.21395.
2. Keum N, Giovannucci E. Global burden of colorectal cancer: emerging trends, risk factors and prevention strategies. *Nat Rev Gastroenterol Hepatol.* 2019;16(12):713–732. doi:10.1038/s41575-019-0189-8.
3. Choi CR, Bakir IA, Hart AL, Graham TA. Clonal evolution of colorectal cancer in IBD. *Nat Rev Gastroenterol Hepatol.* 2017;14(4):218–229. doi:10.1038/nrgastro.2017.1.
4. Lasry A, Zinger A, Ben-Neriah Y. Inflammatory networks underlying colorectal cancer. *Nat Immunol.* 2016;17(3):230–240. doi:10.1038/ni.3384.
5. Zhou CB, Fang JY. The role of pyroptosis in gastrointestinal cancer and immune responses to intestinal microbial infection. *Biochim Biophys Acta Rev Cancer.* 2019;1872(1):1–10. doi:10.1016/j.bbcan.2019.05.001.
6. Wijnands AM, de Jong ME, Lutgens M, Hoentjen F, Elias SG, Oldenburg B, Dutch Initiative on C, Colitis, Prognostic factors for advanced colorectal neoplasia in inflammatory bowel disease: systematic review and meta-analysis. *Gastroenterology.* 2021;160(5):1584–1598. doi:10.1053/j.gastro.2020.12.036.
7. Brenner H, Altenhofen L, Stock C, Hoffmeister M. Prevention, early detection, and overdiagnosis of colorectal cancer within 10 years of screening colonoscopy in Germany. *Clin Gastroenterol Hepatol.* 2015;13(4):717–723. doi:10.1016/j.cgh.2014.08.036.
8. Dow LE, O'Rourke KP, Simon J, Tschaharganeh DF, van Es JH, Clevers H, Lowe SW. Apc restoration promotes cellular differentiation and reestablishes crypt homeostasis in colorectal cancer. *Cell.* 2015;161(7):1539–1552. doi:10.1016/j.cell.2015.05.033.
9. Miller KD, Nogueira L, Devasia T, Mariotto AB, Yabroff KR, Jemal A, Kramer J, Siegel RL. Cancer treatment and survivorship

- statistics, 2022. *CA Cancer J Clin.* 2022;72(5):409–436. doi:10.3322/caac.21731.
10. Linde N, Casanova-Acebes M, Sosa MS, Mortha A, Rahman A, Farias E, Harper K, Tardio E, Reyes Torres I, Jones J, et al. Macrophages orchestrate breast cancer early dissemination and metastasis. *Nat Commun.* 2018;9(1):21. doi:10.1038/s41467-017-02481-5.
 11. Mantovani A, Marchesi F, Malesci A, Laghi L, Allavena P. Tumour-associated macrophages as treatment targets in oncology. *Nat Rev Clin Oncol.* 2017;14(7):399–416. doi:10.1038/nrclinonc.2016.217.
 12. Greten FR, Grivnenikov SI. Inflammation and cancer: triggers, mechanisms, and consequences. *Immunity.* 2019;51(1):27–41. doi:10.1016/j.immuni.2019.06.025.
 13. Caldas C, Brenton JD. Sizing up miRNAs as cancer genes. *Nat Med.* 2005;11(7):712–714. doi:10.1038/nm0705-712.
 14. Schetter AJ, Heegaard NH, Harris CC. Inflammation and cancer: interweaving microRNA, free radical, cytokine and p53 pathways. *Carcinogenesis.* 2010;31(1):37–49. doi:10.1093/carcin/bgp272.
 15. He C, Yu T, Shi Y, Ma C, Yang W, Fang L, Sun M, Wu W, Xiao F, Guo F, et al. MicroRNA 301A promotes intestinal inflammation and colitis-associated cancer development by inhibiting BTG1. *Gastroenterology.* 2017;152(6):1434–1448.e1415. doi:10.1053/j.gastro.2017.01.049.
 16. Polytaichou C, Hommes DW, Palumbo T, Hatzia Apostolou M, Koutsoumpa M, Koukos G, van der Meulen-de Jong AE, Oikonomopoulos A, van Deen WK, Vorvis C, et al. MicroRNA214 is associated with progression of ulcerative colitis, and inhibition reduces development of colitis and colitis-associated cancer in mice. *Gastroenterology.* 2015;149(4):981–992 e911. doi:10.1053/j.gastro.2015.05.057.
 17. Shi C, Yang Y, Xia Y, Okugawa Y, Yang J, Liang Y, Chen H, Zhang P, Wang F, Han H, et al. Novel evidence for an oncogenic role of microRNA-21 in colitis-associated colorectal cancer. *Gut.* 2016;65(9):1470–1481. doi:10.1136/gutjnl-2014-308455.
 18. Li S, Liu Z, Fang XD, Wang XY, Fei BY. 2019. MicroRNA (miR)-597-5p inhibits colon cancer cell migration and invasion by targeting FOS-Like antigen 2 (FOSL2). *Front Oncol.* 9:495. doi:10.3389/fonc.2019.00495.
 19. Chen Z, Ren R, Wan D, Wang Y, Xue X, Jiang M, Shen J, Han Y, Liu F, Shi J, et al. Hsa_circ_101555 functions as a competing endogenous RNA of miR-597-5p to promote colorectal cancer progression. *Oncogene.* 2019;38(32):6017–6034. doi:10.1038/s41388-019-0857-8.
 20. Zlotnik A, Yoshie O. The chemokine superfamily revisited. *Immunity.* 2012;36(5):705–716. doi:10.1016/j.immuni.2012.05.008.
 21. Cui D, Zhao Y, Xu J. Activation of CXCL5-CXCR2 axis promotes proliferation and accelerates G1 to S phase transition of papillary thyroid carcinoma cells and activates JNK and p38 pathways. *Cancer Biol Ther.* 2019;20(5):608–616. doi:10.1080/15384047.2018.1539289.
 22. Zhou SL, Zhou ZJ, Hu ZQ, Li X, Huang XW, Wang Z, Fan J, Dai Z, Zhou J. CXCR2/CXCL5 axis contributes to epithelial-mesenchymal transition of HCC cells through activating PI3K/Akt/GSK-3beta/snail signaling. *Cancer Lett.* 2015;358(2):124–135. doi:10.1016/j.canlet.2014.11.044.
 23. Park YL, Kim HP, Ock CY, Min DW, Kang JK, Lim YJ, Song SH, Han SW, Kim TY. EMT-mediated regulation of CXCL1/5 for resistance to anti-EGFR therapy in colorectal cancer. *Oncogene.* 2022;41(14):2026–2038. doi:10.1038/s41388-021-01920-4.
 24. Zhao J, Ou B, Han D, Wang P, Zong Y, Zhu C, Liu D, Zheng M, Sun J, Feng H, et al. Tumor-derived CXCL5 promotes human colorectal cancer metastasis through activation of the ERK/Elk-1/Snail and AKT/GSK3beta/beta-catenin pathways. *Mol Cancer.* 2017;16(1):70. doi:10.1186/s12943-017-0629-4.
 25. Chen C, Xu ZQ, Zong YP, Ou BC, Shen XH, Feng H, Zheng MH, Zhao JK, Lu AG. CXCL5 induces tumor angiogenesis via enhancing the expression of FOXD1 mediated by the AKT/NF-kappaB pathway in colorectal cancer. *Cell Death Disease.* 2019;10(3):178. doi:10.1038/s41419-019-1431-6.
 26. Rieder F, Fiocchi C. Intestinal fibrosis in inflammatory bowel disease - Current knowledge and future perspectives. *J Crohns Colitis.* 2008;2(4):279–290. doi:10.1016/j.crohns.2008.05.009.
 27. Bai B, Wu F, Ying K, Xu Y, Shan L, Lv Y, Gao X, Xu D, Lu J, Xie B. Therapeutic effects of dihydroartemisinin in multiple stages of colitis-associated colorectal cancer. *Theranostics.* 2021;11(13):6225–6239. doi:10.7150/thno.55939.
 28. Bocchetti M, Ferraro MG, Ricciardiello F, Ottaiano A, Luce A, Cossu AM, Scrima M, Leung WY, Abate M, Stiuso P, et al. The role of microRNAs in development of colitis-associated colorectal cancer. *Int J Mol Sci.* 2021;22(8):3967. doi:10.3390/ijms22083967.
 29. Yashiro M. Ulcerative colitis-associated colorectal cancer. *World J Gastroenterol.* 2014;20(44):16389–16397. doi:10.3748/wjg.v20.i44.16389.
 30. Parang B, Barrett CW, Williams CS. 2016. AOM/DSS model of colitis-associated cancer. *Methods Mol Biol.* 1422:297–307.
 31. Tajasuwan L, Kettawan A, Rungruang T, Wunjuntuk K, Prombutara P, Muangnoi C, Kettawan AK. Inhibitory effect of dietary defatted rice bran in an AOM/DSS-Induced colitis-associated colorectal cancer experimental animal model. *Foods.* 2022;11(21):3488. doi:10.3390/foods11213488.
 32. Francescone R, Hou V, Grivnenikov SI. Cytokines, IBD, and colitis-associated cancer. *Inflamm Bowel Dis.* 2015;21(2):409–418. doi:10.1097/MIB.0000000000000236.
 33. Ho GT, Cartwright JA, Thompson EJ, Bain CC, Rossi AG. Resolution of inflammation and gut repair in IBD: translational steps towards complete mucosal healing. *Inflamm Bowel Dis.* 2020;26(8):1131–1143. doi:10.1093/ibd/izaa045.
 34. Friedrich M, Pohin M, Powrie F. Cytokine networks in the pathophysiology of inflammatory bowel disease. *Immunity.* 2019;50(4):992–1006. doi:10.1016/j.immuni.2019.03.017.
 35. Wei C, Yang C, Wang S, Shi D, Zhang C, Lin X, Liu Q, Dou R, Xiong B. Crosstalk between cancer cells and tumor associated macrophages is required for mesenchymal circulating tumor cell-mediated colorectal cancer metastasis. *Mol Cancer.* 2019;18(1):64. doi:10.1186/s12943-019-0976-4.
 36. Ye L, Zhang T, Kang Z, Guo G, Sun Y, Lin K, Huang Q, Shi X, Ni Z, Ding N, et al. 2019. Tumor-Infiltrating Immune cells Act as a Marker for prognosis in colorectal cancer. *Front Immunol.* 10:2368. doi:10.3389/fimmu.2019.02368.
 37. Bartel DP. MicroRNAs: genomics, biogenesis, mechanism, and function. *Cell.* 2004;116(2):281–297. doi:10.1016/S0092-8674(04)00045-5.
 38. Lee YS, Dutta A. MicroRNAs in cancer. *Annu Rev Pathol.* 2009;4(1):199–227. doi:10.1146/annurev.pathol.4.110807.092222.
 39. Li Q, Lian Y, Deng Y, Chen J, Wu T, Lai X, Zheng B, Qiu C, Peng Y, Li W, et al. 2021. mRNA-engineered mesenchymal stromal cells expressing CXCR2 enhances cell migration and improves recovery in IBD. *Mol Ther Nucleic Acids.* 26:222–236. doi:10.1016/j.omtn.2021.07.009.
 40. Wu S, Yuan W, Luo W, Nie K, Wu X, Meng X, Shen Z, Wang X. miR-126 downregulates CXCL12 expression in intestinal epithelial cells to suppress the recruitment and function of macrophages and tumorigenesis in a murine model of colitis-associated colorectal cancer. *Mol Oncol.* 2022;16(19):3465–3489. doi:10.1002/1878-0261.13218.
 41. Tang A, Li N, Li X, Yang H, Wang W, Zhang L, Li G, Xiong W, Ma J, Shen S. Dynamic activation of the key pathways: linking colitis to colorectal cancer in a mouse model. *Carcinogenesis.* 2012;33(7):1375–1383. doi:10.1093/carcin/bgs183.
 42. Erben U, Loddenkemper C, Doerfel K, Spieckermann S, Haller D, Heimesaat MM, Zeitz M, Siegmund B, Kuhl AA. A guide to histomorphological evaluation of intestinal inflammation in mouse models. *Int J Clin Exp Pathol.* 2014;7(8):4557–4576.